Dynamic Thermal Characteristics of HTS Coil for Conduction-Cooled SMES

Hiroki Kojima, Xin Chen, Naoki Hayakawa, *Member, IEEE*, Fumihiro Endo, *Member, IEEE*, and Hitoshi Okubo, *Member, IEEE*

***Abstract*—In this paper, we investigate the thermal runaway characteristics of a BSCCO HTS single pancake coil conduction-cooled with a 4 K-GM cryo-cooler system. We also evaluate the static and dynamic characteristics of the HTS coil by measuring the temporal evolution of the temperature and the voltage for steady current and the typical current patterns of the load fluctuation compensation at different ambient temperatures T_0 in the range of 20–50 K. Moreover, we experimentally discuss the criterion for monitoring the conduction-cooled HTS SMES system during compensating operation for load fluctuations.**

***Index Terms*—Conduction-cooling, HTS, SMES, thermal runaway.**

I. Introduction

HIGHLY reliable electric power supply units are currently in high demand. Superconducting magnetic energy storage (SMES) systems have high efficiency and fast response times. Therefore, such systems are expected to play a significant role in satisfying the abovementioned demand [1]. In the past few years, SMES systems using conduction-cooled HTS materials together with a cryo-cooler system have been investigated [2]–[6], for their high current density under high magnetic field environments at temperatures lower than 20 K. However, conduction-cooled SMES systems can cause thermal runaway during charging and discharging. For reliable operation of a conduction-cooled HTS SMES system, it is important to understand the thermal and electrical characteristics for preventing thermal runaway.

The stability criterion of the thermal runaway phenomenon in conduction-cooled HTS SMES coils under steady current conditions has been discussed [7]. However, under compensating operation for load fluctuations, the current, the voltage, and the temperature of a SMES coil always change at a frequency of several hertz. Therefore, in order to protect the SMES coil from the risk of thermal runaway during operation, it is necessary to monitor and detect thermal runaway from these time dependent parameters. Although the current margin and the thermal margin are discussed in [7], the quantitative criterion and the overload capacity are needed for monitoring thermal runaway phenomena in HTS SMES coils. We have proposed the criterion for the monitoring of HTS SMES coil under compensating operation for load fluctuations in [8]. However, this criterion has been introduced on the basis of a numerical simulation based on experimental results for the Bi2212 solenoid coil, and therefore we need to confirm its application to other coil configurations.

From the perspective mentioned above, in this paper, we have investigated the thermal runaway characteristics of a conduction-cooled Bi2223 HTS single pancake coil under recovery process in load fluctuation compensating operation. In addition, we have experimentally discussed the criterion of the operating condition below which the thermal stability can be maintained in the recovery process into the standby condition in order to protect an HTS SMES coil from the effect of thermal runaway during the process of load fluctuation compensation.

Manuscript received August 18, 2008. First published June 30, 2009; current version published July 15, 2009.

H. Kojima, N. Hayakawa and F. Endo are with the EcoTopia Science Institute, Nagoya University, Nagoya 464-8603, Japan (e-mail: h-kojima@esi.nagoya-u.ac.jp; nhayakaw@nuee.nagoya-u.ac.jp; endo@esi.nagoya-u.ac.jp).

X. Chen and H. Okubo are with the Department of Electrical Engineering and Computer Science, Nagoya University, Nagoya 464-8603, Japan (e-mail: chinshin@okubo.nuee.nagoya-u.ac.jp; okubo@nuee.nagoya-u.ac.jp).

Color versions of one or more of the figures in this paper are available online at http://ieeexplore.ieee.org.

Digital Object Identifier 10.1109/TASC.2009.2019238

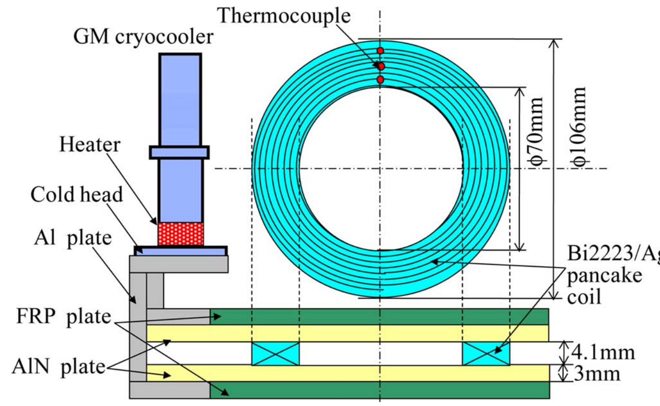

Fig. 1. Arrangement of a single pancake coil sample.

TABLE I
SPECIFICATIONS OF TEST COIL

Material	Bi2223/Ag
Coil inner diameter	70 mm
Coil outer diameter	106 mm
Coil height / Tape width	4.1 mm
Tape thickness	0.21 mm
Number of turns	60 turns
Inductance	0.46 mH
Total length of tape	16.5 m
Magnetic flux density	8.67×10^{-4} T/A at center

II. Experimental Setup

The arrangement and specifications of the test coil are shown in Fig. 1 and Table I, respectively. The test coil is a single pancake coil composed of Bi2223/Ag tape with 60 turns. The tape

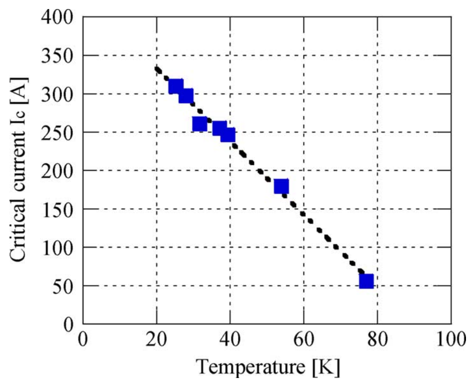

Fig. 2. Critical current I_c as a function of temperature.

width is 4.1 mm, the inner diameter of the coil is 70 mm, and the outer diameter is 106 mm. Polyimide tape is used for insulating the turns. The coil is conduction-cooled with a 4 K-GM cryo-cooler through AlN plates and aluminum plates.

The temperature is measured with 3 thermocouples as indicated in Fig. 1. The operating temperature T_0 of the coil can be controlled to remain in the range between 20 K and 60 K by the heat balance between the cryo-cooler and the heater at the cold head.

III. Fundamental Characteristics

A. Critical Current

We injected steady DC into the coil for 10 s under different values of the operating temperature T_0, and obtained the temperature dependence of the current-voltage characteristics. The critical value for the current I_c was obtained with the criterion of 1 $\mu\mathrm{V/cm}$. Fig. 2 shows the T_0 dependence of I_c, which increases with the decrease of T_0 at a rate of 5 A/K. On the other hand, the n value was almost constant $(n = 8.5)$ under the condition $20\ \mathrm{K} < T_0 < 40\ \mathrm{K}$.

B. Thermal Runaway Characteristics for Steady Current

In this subsection, we measured the thermal runaway characteristics of a conduction-cooled Bi2223/Ag pancake coil at different values of the operating temperature T_0. Fig. 3 shows the temporal evolution of the coil voltage and the temperature for different values of the current I_0 at $T_0 \approx 26$ K. In the case of $I_0 > 240\ \mathrm{A}$, the coil voltage increased within the time range of 20 s. Although the temperature increased even at $I_0 = 200\ \mathrm{A}$, this increase is likely to be due to the heating of the connections between the pancake coil and the current leads.

In [8], we have pointed out that the variation of the resistive coil voltage is preferable for monitoring the thermal runaway. Therefore, we use $\mathrm{d}V/\mathrm{d}t > 0$ within 20 s as a criterion of the thermal runaway in this paper. Fig. 4 shows the temperature dependence of the criterion of the thermal runaway for steady current conditions. At $T_0 \approx 26\ \mathrm{K}$ the criterion of the thermal runaway lies in the range of 200–260 A, which corresponds to about 75% of I_c. At $T_0 \sim 50\ \mathrm{K}$, the criterion of the thermal runaway becomes almost equal to the critical current I_c.

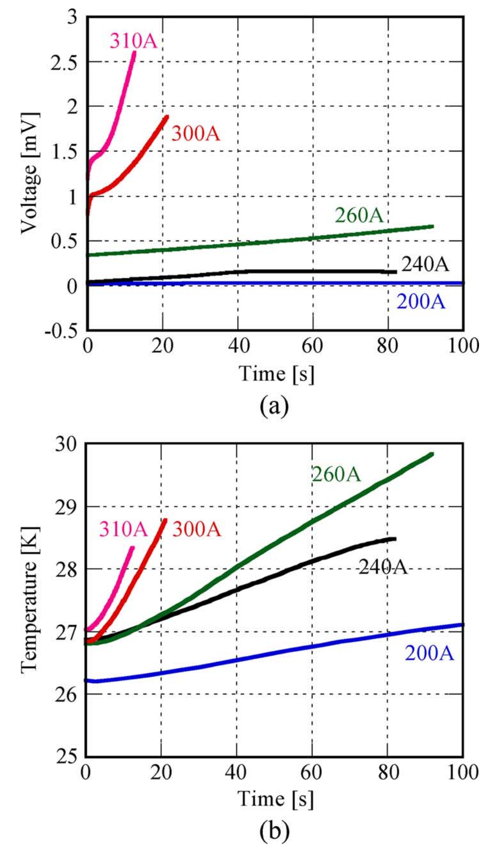

Fig. 3. Temporal evolutions of coil voltage and temperature for different values of the steady current I_0 at operating temperature $T_0 \approx 26\ \mathrm{K}$. (a) Temporal evolutions of coil voltage for different steady current values. (b) Temporal evolutions of average coil temperature for different steady current values.

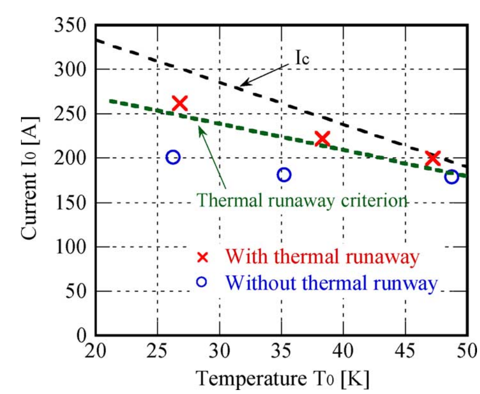

Fig. 4. Thermal runaway criterion for steady current I_0 as a function of the operating temperature T_0.

IV. Criterion of Thermal Runaway During Load Fluctuation Compensating Operation

During the load fluctuation compensation operation, the current, the voltage and the temperature of SMES coil change arbitrarily with time. Now, we consider that the SMES coil has the rated operating values of the temperature T_0 and the current I_0 in the standby condition. The compensating operation completes at certain values for the temperature T_i and the current I_i, and the coil current returns to I_0, as shown in Fig. 5 [8]. If the temperature of the SMES coil returns toward T_0 and the resistive

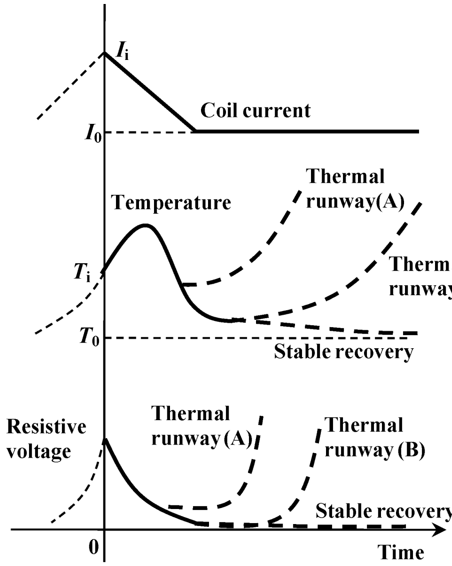

Fig. 5. Pattern of the injected coil current and typical temporal evolution of the temperature and the resistive voltage of the coil for simulating the recovery process in load fluctuation compensating operation.

coil voltage V keeps decreasing, i.e., for $\mathrm{d}V/\mathrm{d}t \leq 0$, such a response can be regarded as stable recovery. On the other hand, if the resistive voltage rises again during the current decay or after reaching I_0, the process can be regarded as thermal runaway. In Fig. 5, the former type of thermal runaway is indicated as "Thermal runaway (A)", and the latter is indicated as "Thermal runaway (B)". Then, as a criterion of a thermal runaway under load fluctuation compensation, we define the upper limit of the operating point (T_i, I_i) as the point at which the thermal stability can be maintained during the recovery process.

In the experiments, T_i can be controlled by the heater and/or the coil current before reaching (T_i, I_i), i.e., for $t < 0$. Here, $\mathrm{d}I/\mathrm{d}t = -20$ A/s was fixed at $T_0 \approx 24$ K. Fig. 6 represents the typical voltage and current variation during the recovery process for $I_0 = 270$ A. In Fig. 6(a), thermal runaway occurs, and $\mathrm{d}V/\mathrm{d}t$ becomes positive during the current decay process toward I_0, i.e., in the case of thermal runaway (A). In the case of Fig. 6(b), $\mathrm{d}V/\mathrm{d}t$ becomes positive after reaching I_0, which indicates that thermal runaway (B) occurs in this condition. Fig. 6(c) shows a typical case of stable recovery, where $\mathrm{d}V/\mathrm{d}t$ keeps decreasing and becomes steady after reaching I_0.

From the results of the above experiments we can determine the criterion of the thermal runaway during load fluctuation compensation, as shown in Fig. 7 for $I_0 = 270$ A at $T_0 = 24$ K. This criterion has a current margin $(I_i - I_0)/I_0$ of 15% for steady current $I_0 = 270$ A at $T_i \sim 34$ K.

Note that in the case of thermal runaway (A), as shown in Fig. 6(a), the thermal runaway occurs before I_0 reaches 270 A. This means that the criterion of thermal runaway at $T_i = 34.4$ K is also applicable to the case of $I_0 < 270$ A since thermal runaway (A) occurs before reaching I_0 even at $I_0 < 270$ A.

Now, we have been able to obtain the criterion of thermal runway during load fluctuation compensation not only by the numerical simulation in [8] but also by the experiments as shown in Fig. 7. These experimental results will be evaluated in detail by modifying the numerical simulation in [8].

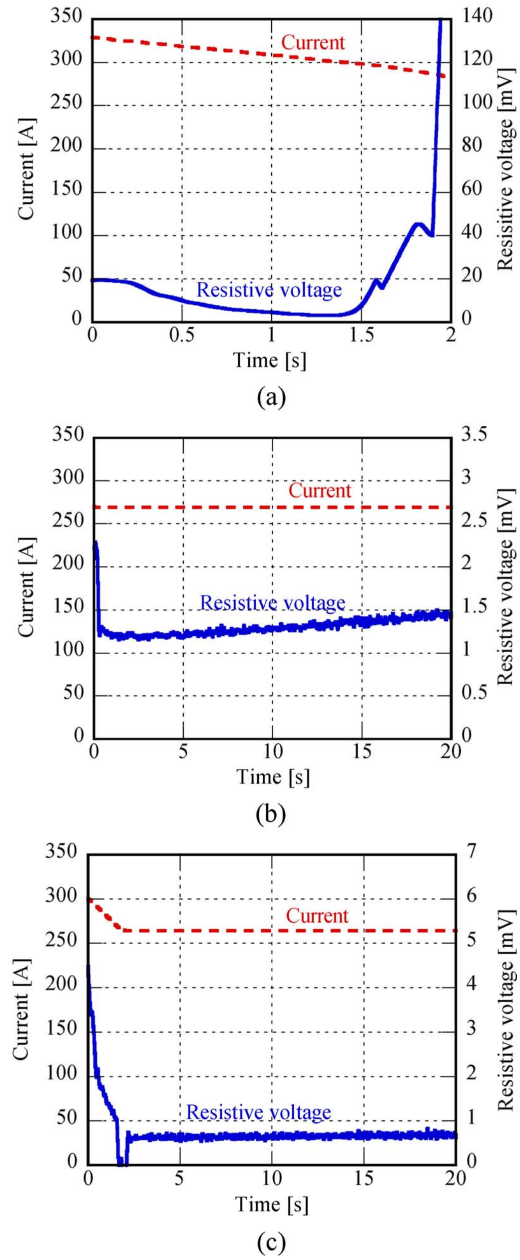

Fig. 6. Temporal evolution of coil current and resistive voltage during the recovery process. (a) Thermal runaway during current decay: Thermal runaway (A) in Fig. 5. ($T_0 = 24$ K, $I_0 = 270$ A, $T_i = 34.4$ K, and $I_i = 330$ A. (b) Thermal runaway after reaching the value of the standby current: Thermal runaway (B) in Fig. 5. ($T_0 = 24$ K, $I_0 = 270$ A, $T_i = 35.6$ K, and $I_i = 270$ A). (c) Stable recovery case. ($T_0 = 24$ K, $I_0 = 270$ A, $T_i = 33.7$ K, and $I_i = 300$ A).

V. Conclusion

In this paper, we have investigated the thermal runaway characteristics of conduction-cooled Bi2223 HTS single pancake coil. We have also discussed the thermal runaway criterion under load fluctuation compensating operation. The main results obtained in this study can be summarized as follows:

1) The temperature dependence of the critical current I_c is observed in the temperature of 20–77 K. The critical current I_c increases with the decrease in temperature at a rate of 5 A/K.

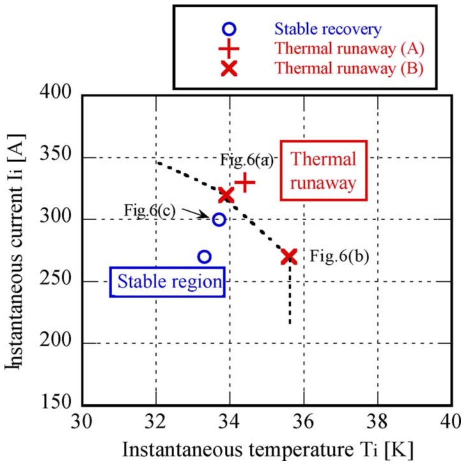

Fig. 7. Thermal runaway characteristics during load fluctuation compensating operation at operating temperature $T_0 = 24$ K, $\mathrm{d}I/\mathrm{d}t = -20$ A/s and $I_0 = 270$ A. Dashed line represents the thermal runaway criterion for standby current $I_0 = 270$ A.

2) The thermal runaway criterion for steady current is determined as a function of the operating temperature T_0. At $T_0 = 26$ K, the criterion of the thermal runaway is about 75% of the critical current I_c.
3) The criterion of the thermal runaway during load fluctuation compensating operation for $\mathrm{d}I/\mathrm{d}t = -20$ A/s at $T_0 = 24$ K is experimentally investigated for the recovery process toward the standby current $I_0 = 270$ A.

REFERENCES

[1] R. Mikkonen, "Highlights of SC power applications in Europe," *IEEE Trans. Applied Superconductivity*, vol. 12, pp. 782–787, Mar. 2002.
[2] B. Bellin, P. Tixador, M. Deleglise, J. C. Vallier, S. Pavard, and C. E. Bruzek, "Cryogenic design of a 800 kJ HTS SMES," *Journal of Physics: Conference Series*, vol. 43, pp. 817–820, 2006.
[3] G. Wojtasiewicz, T. Janowski, S. Kozak, B. Kondratowicz-Kucewicz, J. Kozak, P. Surdacki, and B. A. Glowacki, "HTS magnet for 7.3 kJ SMES system," *Journal of Physics: Conference Series*, vol. 43, pp. 821–824, 2006.
[4] K. C. Seong, H. J. Kim, S. H. Kim, K. D. Sim, M. H. Sohn, E. Y. Lee, S. J. Park, S. Y. Hahn, and M. W. Park, "Development of a 600 kJ HTS SMES," *Physica C*, to be published.
[5] A. Ishiyama, M. Yanai, T. Morisaki, H. Ueda, S. Akita, S. Kouso, Y. Tatsuta, H. Abe, and K. Tasaki, "Transient thermal characteristics of cryocooler-cooled HTS coil for SMES," *IEEE Trans. Applied Superconductivity*, vol. 15, pp. 1879–1882, Jun. 2005.
[6] S. Nagaya, N. Hirano, H. Moriguchi, K. Shikimachi, H. Nakabayashi, S. Hanai, J. Inagaki, S. Ioka, and S. Kawashima, "Field test results of the 5 MVA SMES system for bridging instantaneous voltage dips," *IEEE Trans. Applied Superconductivity*, vol. 16, pp. 632–635, Jun. 2006.
[7] A. Ishiyama and H. Asai, "A stability criterion for cryocooler-cooled HTS coils," *IEEE Trans. Applied Superconductivity*, vol. 11, pp. 1832–1835, Mar. 2001.
[8] H. Kojima, N. Hayakawa, S. Noguchi, F. Endo, N. Hirano, S. Nagaya, and H. Okubo, "Thermal runaway characteristics of Bi2212 coil for conduction-cooled SMES," *IEEE Trans. Applied Superconductivity*, vol. 17, pp. 1959–1962, 2007.